Japanese Journal of Applied Physics **57**, 058002 (2018)
https://doi.org/10.7567/JJAP.57.058002

BRIEF NOTE

Displacement sensing based on modal interference in polymer optical fibers with partially applied strain

Yosuke Mizuno*, Sonoko Hagiwara, Tomohito Kawa, Heeyoung Lee, and Kentaro Nakamura

Institute of Innovative Research, Tokyo Institute of Technology, Yokohama 226-8503, Japan

*E-mail: ymizuno@sonic.pi.titech.ac.jp

Received January 22, 2018; accepted March 5, 2018; published online April 13, 2018

Strain sensing based on modal interference in multimode fibers (MMFs) has been extensively studied, but no experimental or theoretical reports have been given as to how the system works when strain is applied not to the whole MMF but only to part of the MMF. Here, using a perfluorinated graded-index polymer optical fiber as the MMF, we investigate the strain sensing characteristics of this type of sensor when strain is partially applied to fiber sections with different lengths. The strain sensitivity dependence on the length of the strained section reveals that this strain sensor actually behaves as a displacement sensor. © 2018 The Japan Society of Applied Physics

To develop smart materials and structures, strain sensing using optical fibers has been regarded as one of the major research targets, and its various configurations have been reported thus far. Their operating principles include fiber Bragg gratings,[1–4] long-period gratings,[5–7] Brillouin scattering,[8–13] Raman scattering,[14–16] optical interference,[17–30] and many others. Among numerous types of interference-based strain sensors, those based on the interference of multiple guided modes in multimode fibers (MMFs) have recently attracted considerable attention because they generally offer system simplicity, cost efficiency, and high sensitivity. Many multimode-interference-based configurations have been developed, as listed in Table I in Ref. 18. Here, we focus on the most widely used simple configuration, which is often referred to as a "single-mode-multimode-single-mode" (SMS) structure.[19–28] This means that an MMF, which works as a sensing fiber, is placed between two single-mode fibers (SMFs).

The first demonstration of SMS-based strain sensing was given by Liu et al.[19] Using a 1.8-m-long silica graded-index (GI-) MMF, they reported a strain sensitivity of $-18.6\,\mathrm{pm}/\mu\varepsilon$ at 1550 nm. Then, Tripathi et al.[20] clarified that not only the absolute value but also the sign of the strain sensitivity is determined by a so-called "critical wavelength", which depends on the structural and material properties of the MMF. In order to extend the strain dynamic range, Huang et al.[21] used a 0.16-m-long poly(methyl methacrylate) (PMMA)-based step-index polymer optical fiber (POF) as an MMF and obtained a strain sensitivity of $-1.72\,\mathrm{pm}/\mu\varepsilon$ at 1570 nm. The propagation loss of PMMA-based POFs is, however, so high at telecommunication wavelength ($\gg$100 dB/m) that the measurement range is inherently limited to $\ll$1 m. One solution to tackle this issue is to employ a perfluorinated (PF) GI-POF[31–36] as an MMF, which is the only POF with a relatively low loss of ~0.25 dB/m even at 1550 nm (or ~0.05 dB/m at 1300 nm). Numata et al.[22] implemented an SMS-based strain sensor using a 1.0-m-long PFGI-POF and obtained a strain sensitivity of $-112\,\mathrm{pm}/\mu\varepsilon$ (core diameter: 62.5 μm) at 1300 nm. Its absolute value is much larger than those of previous reports using other MMFs.

In addition to these advances, to date, significant efforts have been made to improve the performance of SMS-based strain sensors.[23,24,26–28] One report has clarified that the strain sensitivity of an SMS-based sensor does not depend on the length of the MMF to be strained.[27] This fact indicates that not only two fundamental modes but also many other modes need to be simultaneously considered to elucidate the performance of this type of sensor (as is also inferred by the existence of the critical wavelength).[20] In the meantime, no reports have been published to clarify the operation of the system when strain is applied not to the whole length of the MMF but only to part of the MMF. It is highly conceivable that, when we monitor the distortion of a structure in which an MMF is embedded, strain is partially applied to the MMF. Thus, it is of paramount importance to clarify this point.

In this work, using a PFGI-POF as an MMF, we investigate the performance of the SMS-based strain sensor when strain is partially applied to fiber sections with different lengths. The strain sensitivity plotted as a function of the length of the strained section reveals that, whether strain is applied to the whole length of the MMF or only to part of the MMF, the SMS-based strain sensors can be treated as displacement sensors.

Here, we present a simplified explanation of the operating principle of SMS-based strain sensing. When light is injected from the first SMF into the MMF, multiple guided modes are excited and travel along the MMF with their respective propagation constants. At the other MMF-to-SMF boundary, the net field coupled to the second SMF is determined by the relative phase differences among all the guided modes. If we simply assume that the MMF and the two SMFs are perfectly axially aligned, the optical output power from the second SMF, P_{out}, can be given as[25]

$$P_{\mathrm{out}} = |a_0^2 + a_1^2 \exp i(\beta_0 - \beta_1)L + a_2^2 \exp i(\beta_0 - \beta_2)L + \cdots|^2, \quad (1)$$

where a_j is the field amplitudes of the j-th modes at the first SMF-to-MMF boundary, β_j is the propagation constants of the j-th modes, and L is the length of the MMF. It is clear that P_{out} is influenced by strain applied to the MMF (which causes some change in β_j and L), and it is thus feasible to perform strain sensing by measuring the shift of spectral dips or peaks.

The MMF used in the experiment is a 1.0-m-long PFGI-POF.[31–36] It has a core diameter of 62.5 μm, a cladding diameter of 72.5 μm, and an overcladding diameter of 750 μm. The core and cladding layers are made up of doped and undoped polyperfluorobutenylvinyl ether [refractive indices: 1.356 (center) and 1.342], respectively, while the overcladding layer for protecting the core and cladding layers is composed of polycarbonate.

The experimental setup of the SMS-based strain sensing using the PFGI-POF is depicted in Fig. 1. The output of a supercontinuum source (SCS) with a bandwidth of 460–

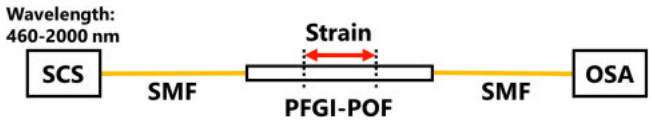

Fig. 1. (Color online) Experimental setup. OSA: optical spectrum analyzer; PFGI-POF: perfluorinated graded-index polymer optical fiber; SCS: supercontinuum source; SMF: single-mode fiber.

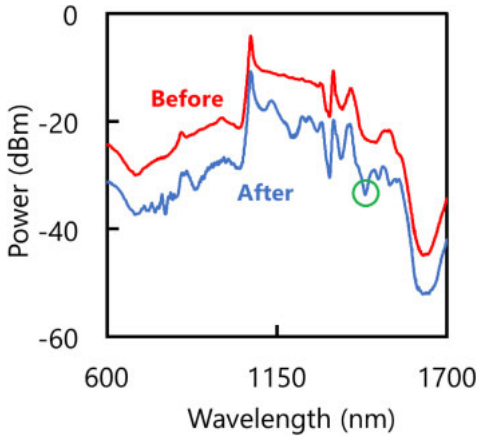

Fig. 2. (Color online) Optical spectra measured before and after the transmission through the POF. The spectral dip in the green circle was used in the subsequent measurements.

2000 nm was injected into one end of the PFGI-POF. The SMF-to-POF coupling was performed using so-called butt-coupling.[32] The transmitted light was injected into an SMF and then guided to an optical spectrum analyzer (OSA) with a bandwidth of 600–1700 nm. The whole setup was fixed during all measurements, which led to a negligible change in the polarization state (guaranteed by the fact that almost the same spectral patterns were constantly observed). Strain was applied partially to the middle of the PFGI-POF using translation stages. The lengths of the strained sections were set to 0.1, 0.2, 0.4, 0.6, 0.8, and 0.93 m (note that 0.93 m is the length of the whole POF excluding the connectors at both ends). Regardless of the lengths of the strained sections, the same amount of displacement of up to 500 μm was applied.

We first measured and compared the optical spectra before and after the transmission through the POF, namely, those of the SCS output and the OSA input (Fig. 2). The optical power at each wavelength was reduced by ∼7.7 dB mainly because of the propagation loss of the POF. The spectrum after the POF transmission exhibited some dips; as these dips were not observed in the spectrum before the POF transmission, it is clear that they were induced by the modal interference in the POF. Considering that the extremely clear dips around 1300 nm are caused not by the modal interference but by the inherent property of the SCS, we used the relatively clear dip at 1470 nm in the following measurements.

Subsequently, we measured the spectral change around 1470 nm when a displacement of up to 500 μm was applied to a 0.1-m-long section in the middle of the POF (corresponding to partially applied strain of up to 0.5%). As shown in Fig. 3(a), with increasing displacement, the dip shifted to shorter wavelength. The dip wavelength dependence on displacement was almost linear [Fig. 3(b)], and its dependence coefficient (with displacement converted into strain) was

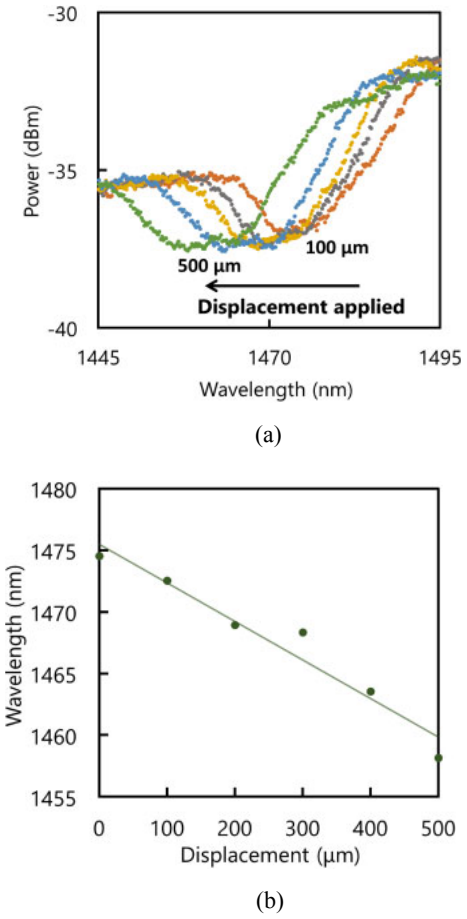

Fig. 3. (Color online) (a) Applied displacement dependence of the spectral dip at 1470 nm when the length of the strained section was 0.1 m. (b) Corresponding dip wavelength plotted as a function of displacement. The solid line is a linear fit.

−3.1 pm/με. We also measured the spectral change when displacement was applied to POF sections with different lengths. The example results, i.e., the spectral dependence and dip wavelength dependence on displacement when the length of the strained section was 0.93 m, are shown in Figs. 4(a) and 4(b), respectively. As displacement was increased, the dip shifted to shorter wavelength with a dependence coefficient of −48 pm/με. Its absolute value is 2.3 times smaller than that of our previous report[22] because not only the strained length but also the measured wavelength region was largely different.

Finally, the absolute value of the measured strain sensitivity was plotted as a function of the length of the strained section (Fig. 5). The sensitivity was almost proportional to the strained length with a coefficient of 51.7 pm/με/m. This result indicates that, regardless of the strain magnitude or the strained length, the spectral dip shifts for the same amount of wavelength, as long as the displacement of the POF is constant. This feature is not a matter of course, considering that the strain sensitivity does not explicitly depend on the POF length (when strain is applied to the whole length) and that all the guided modes in the POF need to be simultaneously considered to explain the behavior of this sensor. Additional discussion based on a "refocusing length" of a GI-MMF[37] is provided in the online supplementary data at http://stacks.iop.org/JJAP/57/058002/mmedia. Thus, we proved that, even including the case where strain is applied only to part of the POF, SMS-based "strain" sensing can be

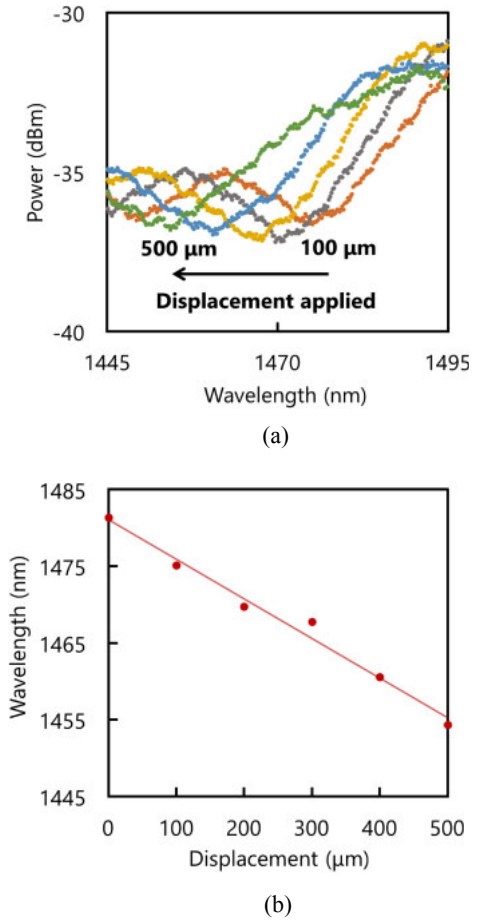

Fig. 4. (Color online) (a) Applied displacement dependence of the spectral dip at 1470 nm when the length of the strained section was 0.93 m. (b) Corresponding dip wavelength plotted as a function of displacement. The solid line is a linear fit.

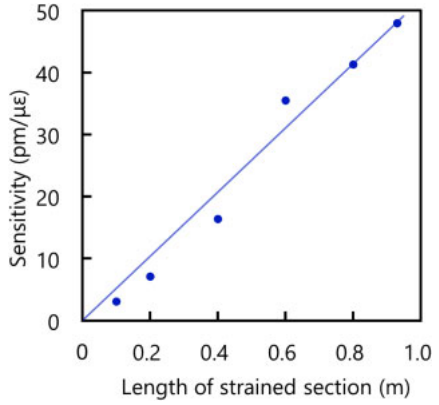

Fig. 5. (Color online) Measured strain sensitivity (absolute value) plotted as a function of the length of the strained section. The solid line is a linear fit.

treated as "displacement" sensing; note that a strain sensor using the whole length of the fiber is naturally treated as a displacement sensor, as strain and displacement are in one-to-one correspondence in this case.

In conclusion, we characterized the SMS-based strain sensor using a PFGI-POF when strain was partially applied to fiber sections with different lengths, and the strain sensitivity was found to be proportional to the length of the strained section. This result indicates that, whether strain is applied to the whole length of the POF or only to part of the POF, the SMS-based strain sensors can be treated as displacement sensors. We believe that this finding will be a basic but important guideline when we practically use SMS-based strain sensors to monitor the conditions of civil structures in the future.

Acknowledgments This work was supported by JSPS KAKENHI Grant Numbers 17H04930 and 17J07226, and by research grants from the Japan Gas Association, the ESPEC Foundation for Global Environment Research and Technology, the Association for Disaster Prevention Research, the Fujikura Foundation, and the Japan Association for Chemical Innovation.

1) A. D. Kersey, M. A. Davis, H. J. Patrick, M. LeBlanc, K. P. Koo, C. G. Askins, M. A. Putnam, and E. J. Friebele, J. Lightwave Technol. **15**, 1442 (1997).
2) J. Jung, H. Nam, B. Lee, J. O. Byun, and N. S. Kim, Appl. Opt. **38**, 2752 (1999).
3) B. O. Guan, H. Y. Tam, X. M. Tao, and X. Y. Dong, IEEE Photonics Technol. Lett. **12**, 675 (2000).
4) Y. Zhang and W. Yang, Sens. Actuators A **239**, 185 (2016).
5) V. Bhatia and A. M. Vangsarkar, Opt. Lett. **21**, 692 (1996).
6) Y. P. Wang, L. X. Xiao, D. N. Wang, and W. Jin, Opt. Lett. **31**, 3414 (2006).
7) P. Wang, L. Xian, and H. Li, IEEE Photonics Technol. Lett. **27**, 557 (2015).
8) T. Kurashima, T. Horiguchi, H. Izumita, S. Furukawa, and Y. Koyamada, IEICE Trans. Electron. **E76-C**, 382 (1993).
9) Y. Dong, D. Ba, T. Jiang, D. Zhou, H. Zhang, C. Zhu, Z. Lu, H. Li, L. Chen, and X. Bao, IEEE Photonics J. **5**, 2600407 (2013).
10) T. Horiguchi and M. Tateda, J. Lightwave Technol. **7**, 1170 (1989).
11) K. Hotate and T. Hasegawa, IEICE Trans. Electron. **E83-C**, 405 (2000).
12) Y. Mizuno, W. Zou, Z. He, and K. Hotate, Opt. Express **16**, 12148 (2008).
13) Y. Mizuno, N. Hayashi, H. Fukuda, K. Y. Song, and K. Nakamura, Light: Sci. Appl. **5**, e16184 (2016).
14) M. A. Farahani and T. Gogolla, J. Lightwave Technol. **17**, 1379 (1999).
15) M. N. Alahbabi, Y. T. Cho, and T. P. Newson, Opt. Lett. **30**, 1276 (2005).
16) M. K. Saxena, S. D. V. S. J. Raju, R. Arya, R. B. Pachori, S. V. G. Ravindranath, S. Kher, and S. M. Oak, Opt. Laser Technol. **65**, 14 (2015).
17) Y. J. Rao, D. A. Jackson, L. Zhang, and I. Bennion, Opt. Lett. **21**, 1556 (1996).
18) O. Frazão, S. O. Silva, J. Viegas, L. A. Ferreira, F. M. Araújo, and J. L. Santos, Appl. Opt. **50**, E184 (2011).
19) Y. Liu and L. Wei, Appl. Opt. **46**, 2516 (2007).
20) S. M. Tripathi, A. Kumar, R. K. Varshney, Y. B. P. Kumar, E. Marin, and J. P. Meunier, J. Lightwave Technol. **27**, 2348 (2009).
21) J. Huang, X. Lan, H. Wang, L. Yuan, T. Wei, Z. Gao, and H. Xiao, Opt. Lett. **37**, 4308 (2012).
22) G. Numata, N. Hayashi, M. Tabaru, Y. Mizuno, and K. Nakamura, IEEE Photonics J. **6**, 6802306 (2014).
23) G. Numata, N. Hayashi, M. Tabaru, Y. Mizuno, and K. Nakamura, IEICE Electron. Express **12**, 20141173 (2015).
24) G. Numata, N. Hayashi, M. Tabaru, Y. Mizuno, and K. Nakamura, Appl. Phys. Express **8**, 072502 (2015).
25) A. Kumar, R. K. Varshney, C. S. Antony, and P. Sharma, Opt. Commun. **219**, 215 (2003).
26) M. Kumar, A. Kumar, and S. M. Tripathi, Opt. Commun. **312**, 222 (2014).
27) T. Kawa, G. Numata, H. Lee, N. Hayashi, Y. Mizuno, and K. Nakamura, IEICE Electron. Express **14**, 20161239 (2017).
28) T. Kawa, G. Numata, H. Lee, N. Hayashi, Y. Mizuno, and K. Nakamura, Jpn. J. Appl. Phys. **56**, 078002 (2017).
29) A. Mehta, W. Mohammed, and E. G. Johnson, IEEE Photonics Technol. Lett. **15**, 1129 (2003).
30) E. Li, X. Wang, and C. Zhang, Appl. Phys. Lett. **89**, 091119 (2006).
31) Y. Koike and M. Asai, NPG Asia Mater. **1**, 22 (2009).
32) Y. Mizuno and K. Nakamura, Appl. Phys. Lett. **97**, 021103 (2010).
33) Y. Dong, P. Xu, H. Zhang, Z. Lu, L. Chen, and X. Bao, Opt. Express **22**, 26510 (2014).
34) A. Minardo, R. Bernini, and L. Zeni, IEEE Photonics Technol. Lett. **26**, 387 (2014).
35) N. Hayashi, Y. Mizuno, and K. Nakamura, J. Lightwave Technol. **32**, 3999 (2014).
36) H. Lee, N. Hayashi, Y. Mizuno, and K. Nakamura, J. Lightwave Technol. **35**, 2306 (2017).
37) G. P. Agrawal, *Fiber-Optic Communication Systems* (Wiley-VCH, Weinheim, 2010).

Supplementary Information

Displacement sensing based on modal interference in polymer optical fibers with partially applied strain

Yosuke Mizuno*, Sonoko Hagiwara, Tomohito Kawa, Heeyoung Lee, and Kentaro Nakamura

Institute of Innovative Research, Tokyo Institute of Technology, Yokohama 226-8503, Japan

*E-mail: ymizuno@sonic.pi.titech.ac.jp

Discussion

We discuss how we can reasonably explain the apparently contradictory results of the previous report (the strain sensitivity (and the dip shift as well) does not explicitly depend on the MMF length)[27] and this paper (the dip shift clearly depends on the MMF length (because the dip shift is proportional to the displacement)). What is important here is a "refocusing length" of a GI-MMF, which is the period of the continual refocusing of the rays in the core. The refocusing length L_{ref} can be calculated using the core radius a (62.5 μm / 2) and the refractive indices of the core (center) n_1 and the cladding n_2 (which are 1.356 and 1.342, respectively) as:[37] $L_{\mathrm{ref}} = \pi a\sqrt{2/(1-n_2/n_1)}$, which is 1366 μm in this experiment. In the SMS-based measurement, similar transmitted spectra are repeatedly obtained when the MMF is elongated by multiples of the refocusing length, as experimentally shown in Figs. S1(a)–(d) and S2. In the measurements in this paper, displacements (changed continuously from 0 up to 500 μm) were applied to part of the GI-MMF. As a result, an identical spectral dip (corresponding to the same modal conditions) around 1470 nm was tracked, leading to the clear dependence of the dip shift on the MMF length. In contrast, in the measurements in the previous report,[27] the strain sensitivity around 1310 nm was investigated when the MMF length was discontinuously set to 0.3, 0.7, 1.0, and 2.0 m (note that each difference is much longer than the refocusing length). Considering that similar spectra are repeatedly obtained when the MMF length is changed by multiples of the refocusing length, even when spectral dips are observed in the same wavelength region, they may not correspond to the same modal conditions. In general, the dips corresponding to different modal conditions have different strain sensitivities even when observed in the same wavelength region (see Figs. S3(a),(b)). Therefore, it is reasonable that, in the previous report,[27] the strain sensitivity did not explicitly depend on the MMF length, unlike in this paper.

Supplementary Figures

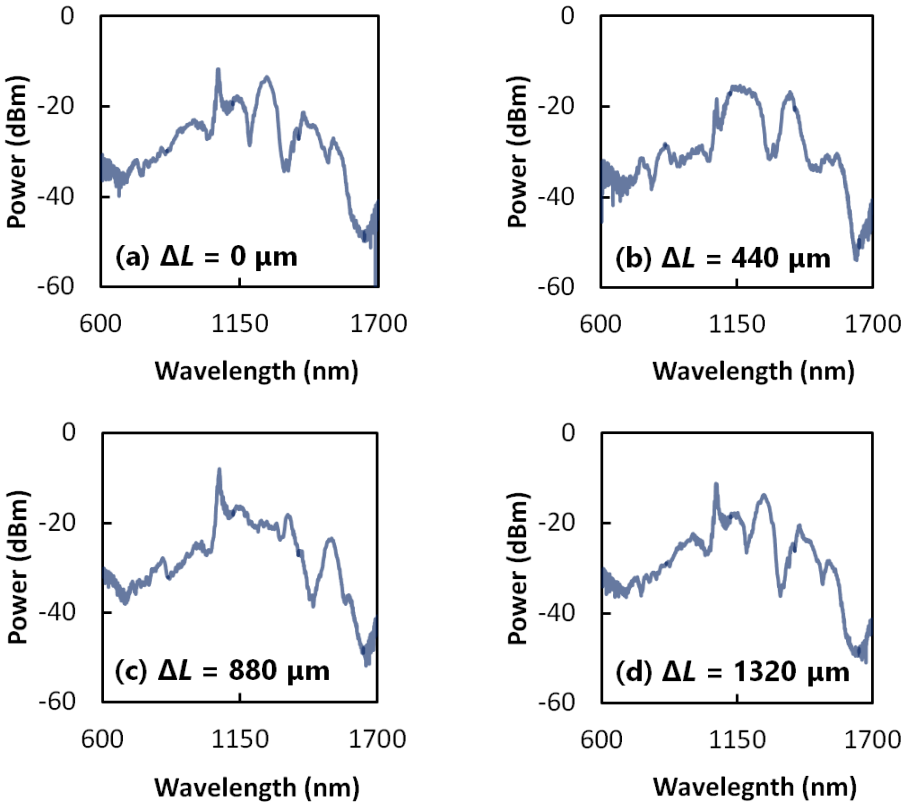

Supplementary Figure S1 | Transmitted optical spectra when displacements ΔL of (a) 0, (b) 440, (c) 880, and (d) 1320 μm were applied to the whole length of a 0.5-m-long PFGI-POF. Note that the spectrum of (a) has a marked similarity to that of (d).

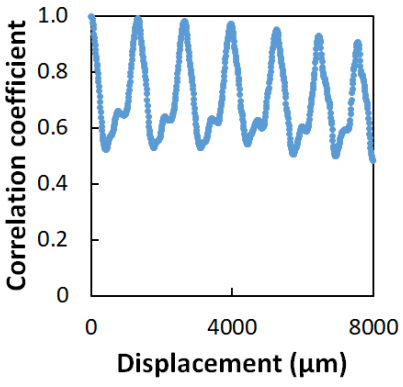

Supplementary Figure S2 | Pearson correlation coefficient (calculated using the data in the wavelength range from 800 to 1600 nm) plotted as a function of displacement. This clearly shows that similar spectra were repeatedly observed when the MMF was elongated by multiples of approximately 1320 μm (which is close to the refocusing length).

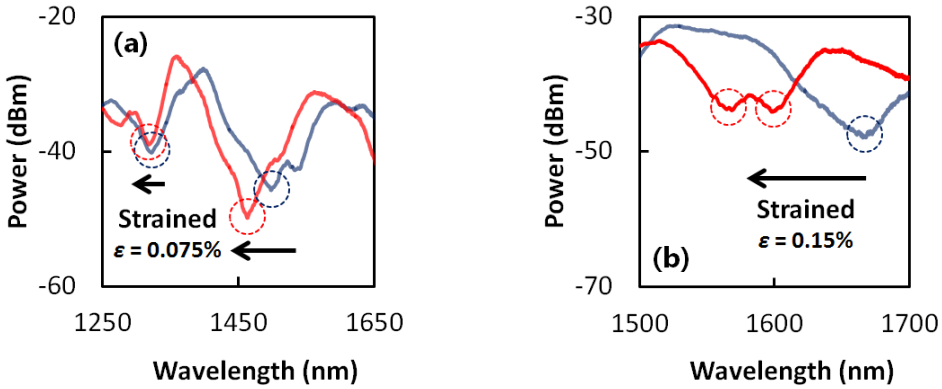

Supplementary Figure S3 | (a,b) Examples of the spectral dependences on strain.